Journal of
Applied Crystallography
ISSN 0021-8898

Received 11 November 2005
Accepted 9 March 2006

The determination of pore volumes, pore shapes and diffusion paths in microporous crystals

Horst Küppers,[a]* Friedrich Liebau[a] and Anthony L. Spek[b]

[a]Institut für Geowissenschaften der Universität Kiel, D-24098 Kiel, Germany, and [b]Section of Crystal and Structural Chemistry, Faculty of Science, University of Utrecht, Padualaan 8, NL-3584 CH Utrecht, The Netherlands. Correspondence e-mail: kueppers@min.uni-kiel.de

The original option *SOLV* of the program *PLATON*, which is primarily devoted to the study of organic structures, has been extended to studies of microporous inorganic crystals. The space that is available for a potential spherical guest within a pore can be regarded as being outlined by rolling a sphere of the guest's radius over the surfaces of the host atoms that form the pore. The volumes of the pores are determined in Å^3 and the pore shapes can be drawn. The pore volumes of several microporous phases have been calculated and compared with results obtained with other methods. An essential feature of the program is the option to vary a parameter called 'probe radius', which models the size of a guest. The decision whether a void is a pore or not and the dimensionality of a pore depend on the radius of the guest, which is approximated by a sphere. This is demonstrated for the structure of the zeolite afghanite. With decreasing probe radius, cages can coalesce into larger cages and finally into channels and channel systems. The variation of the probe radius allows one to determine whether a window between adjacent pores is permeable to guests; in addition, diffusion paths in zeolites and zeolite-like structures can be determined and visualized.

1. Introduction

Among crystals with low packing density, those exhibiting larger voids (micropores), which are able to accommodate guests, are of special interest in various industrial applications. In particular, clathrates, zeolites and zeolite-like materials are of great technical importance. Therefore, a description of the pores, their size, shape and ability to incorporate certain guests, including reaction intermediates and reaction products, is desirable. The possibility that guests can use pores as diffusion paths is of essential practical significance. To avoid misunderstandings, a recollection of terms follows.

In porous materials, distinction is made between 'host atoms' and 'guests' (atoms, molecules or ions) that may be located in the pores. The bonds between the host atoms are stronger than the bonds between host atoms and guests.

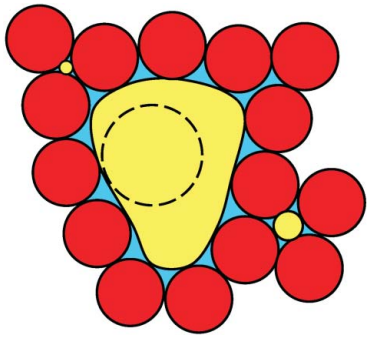

Figure 1
Schematic representation of void and cusp areas in a hypothetical two-dimensional structure. Host atoms red, void areas yellow, cusp areas blue, circular guest atom dashed.

For simple crystal structure models, atoms are assumed to have spherical shape, and to each atom species, i, a certain atomic radius, r_i, is assigned. Thus, certain parts of the structure are 'filled with matter' while others are 'empty'. The empty space can be subdivided according to the following scheme and Fig. 1.

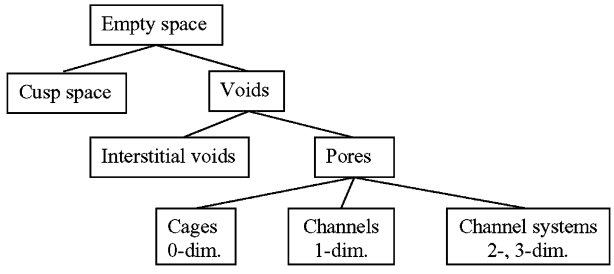

In Fig. 1 a simple two-dimensional example is shown, in which circular host atoms of equal size are drawn in red and empty space in yellow and blue. Within the empty space, subspaces can be distinguished, each of which can be characterized by a circle that is fixed by contact with at least three host atom circles. These subspaces are called 'voids' (yellow areas in Fig. 1). If all voids are subtracted from the empty space, subspaces remain (blue areas in Fig. 1), which we call 'cusps'. In the two-dimensional structure, these cusps are finite

and curved triangles if the host-atom circles are in contact with each other. In the three-dimensional case, a void can be characterized by a sphere that is fixed by contacts with at least four atom spheres. Examples of such voids are the tetrahedral and octahedral interstices in closest sphere packings with four and six touching spheres, respectively. In three dimensions, the cusps are no longer finite regions, but they are interconnected and form a porous three-dimensional 'cusp space'.

In porous materials, only larger voids that are able to accommodate guests are of interest. Such voids are called 'pores', whereas smaller voids are called 'interstitial voids'. In the two-dimensional structure of Fig. 1, the small yellow circles between three or four atoms are examples of interstitial voids. The large yellow void in the centre of Fig. 1, which is able to accommodate a guest (dashed circle), represents a pore. Evidently, the decision whether a void is a pore or an interstitial void depends on the size of a potential guest. A pore is defined as 'a void, which can accommodate a guest of a given size and shape'. To be independent of the specific shape, the guest is assumed to be a sphere. The size of the pore can be characterized by the diameter of the maximum sphere which can be accommodated by the pore.

This proposed definition of a pore is not in accordance with the recommended definition given by the IUPAC (McCusker *et al.*, 2001) according to which a void is a pore 'if it has a free volume larger than that of a sphere with a 2.5 Å diameter'. In the present paper it will be shown that our new definition seems to be a more appropriate one.

Pores can be subdivided with respect to their dimensionality. A pore is called a 'cage' if it has finite extension (pore dimensionality $D^{\rm p} = 0$), a 'channel' if the pore has infinite extension in one direction ($D^{\rm p} = 1$) and a 'channel system' if the pore has infinite extension in more than one direction ($D^{\rm p} = 2, 3$).

Ordered microporous materials with inorganic hosts ('poroates') are called 'clathrates' if they contain only pores with $D^{\rm p} = 0$, and 'zeoates' if they contain pores with $D^{\rm p} > 0$ (Liebau, 2003).

The porosity P of a porous material is defined as the ratio of the sum of the volumes of the pores per unit cell, $\sum_i V_i^{\rm p}$, and the unit-cell volume, $V_{\rm uc}$,

$$\mathsf{P} = \sum_i V_i^{\rm p}/V_{\rm uc}. \qquad (1)$$

In order to calculate P, it is necessary to determine the volumes of the individual pores, $V_i^{\rm p}$. Of the several methods to calculate $V^{\rm p}$ which have been proposed, the following are mentioned.

(i) Blatov *et al.* (2005) describe the space of a pore as a conglomerate of Voronoi–Dirichlet polyhedra. In their method, parts of the cusp space that cannot be occupied by a potential guest are included in the pore volume. A further disadvantage of this method is the neglect of the chemical nature of host and guest atoms, which, as shall be shown in §§3 and 4, has a considerable influence on the volume of the pores.

(ii) Marler (1989) (see also Liebau, 2003) approximates the volume of a cage by fitting an ellipsoid to the inner wall of the cage and approximates the channel volume by fitting a cylinder to the inner wall of the channel. With this method, deviations from ellipsoidal or cylindrical shape, namely depressions and protrusions, are not taken into account.

(iii) In his program *PLATON*, Spek (2005) presents an option, *SOLV*, to detect pores and to describe their geometrical properties. Using *SOLV*, one can calculate the volumes of pores of any shape. The method can, in addition, be used to determine diffusion paths in zeoates, as shall be shown in §4.

The *SOLV* routine was originally and primarily developed to search for pores in organic materials that can incorporate water or other solvate molecules. It appears that this routine has been applied so far only rarely and not specifically to zeolites and other similar inorganic materials. The present paper describes the application of the *SOLV* routine, which is extended to investigate the microporous nature of poroates with inorganic hosts. It turns out that variation of the probe radius, which in studies of crystals with organic hosts was used as a constant parameter, allows extensive predictions to be made on the geometrical properties of microporous materials, such as pore volumes, pore shapes and diffusion paths.

2. Description of the *SOLV* option of the *PLATON* program

In Fig. 2, the *SOLV* algorithm is visualized and explained with the aid of a two-dimensional hypothetical structure with host atoms of different size. In three dimensions, the host atoms are represented by spheres with radii r_i, which, in the two-

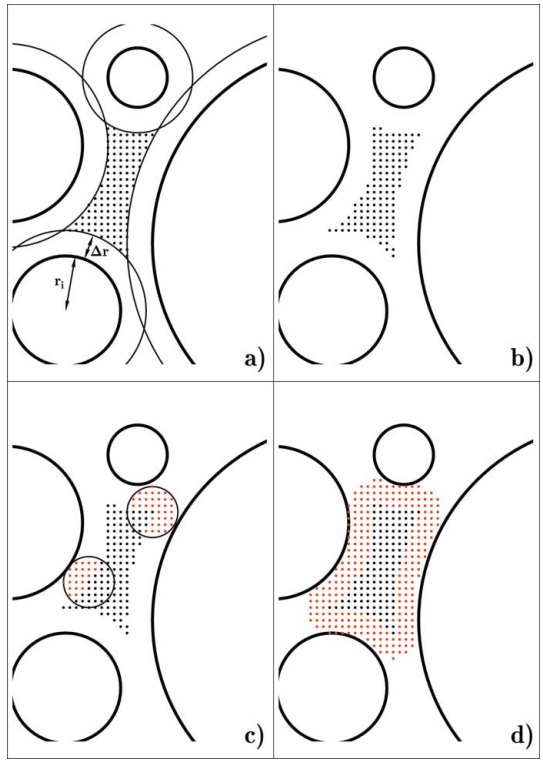

Figure 2
Two-dimensional illustration of the steps to determine pore volumes with *SOLV*. For details see text.

dimensional illustration of Fig. 2, are drawn as circles. In the first step, 'extended spheres' (circles) of radii $r_i + \Delta r$ are drawn around the centres of the host atoms (Fig. 2*a*). The increment Δr is called the 'probe radius'.

In the second step, the unit cell of the structure is superimposed with a fine-meshed lattice of grid points. The distance of the grid points is much smaller than the size of the unit-cell axis. Grid points that do not belong to any of the extended spheres (circles) will make up a primary 'cloud of grid points' (CGP) (Fig. 2*b*). Such clouds will be found only in the middle of voids of sufficient size to house a guest, because each grid point has a distance of at least Δr from each of the surfaces of the surrounding host atoms. By this procedure, it is prevented that grid points can be located in interstitial voids. Since, at this stage, a CGP does not yet fill the total space available for a potential guest, the CGP is augmented to the whole available space by the following procedure: spheres (circles) of radius Δr are drawn around each grid point of the primary CGP, and grid points, lying within these spheres (circles) and not yet being part of the CGP, are added to the CGP. This extended set of grid points constitutes the final 'augmented CGP'. To visualize this step, in Fig. 2(*c*) two such circles with their new grid points (red dots) are shown. The augmented CGP will now be in contact with the surrounding host atoms and will represent the space available to a guest of radius Δr, thus describing the pore (Fig. 2*d*).

The pore space can, as well, be regarded as being outlined by rolling a sphere (circle) of radius Δr over the surfaces of the host atoms.

The volume (area) of the pore, $V^{\rm p}$, can now be determined simply by adding up the number of grid points within the pore. Furthermore, the augmented CGP gives information on the shape of the pore, which generally deviates from spherical (circular) or ellipsoidal (elliptic) shape. This may be important with respect to the shape of potential non-spherical guests.

In order to characterize a pore, *SOLV* provides the following features to calculate (*a*) the centre of gravity of the grid points of the CGP, (*b*) the volume of the pore in Å^3, (*c*) the second moment of the distribution of the grid points (represented by an ellipsoid), (*d*) distances from the centre of gravity to the centres of the host atoms surrounding the pore, and (*e*) graphical representations in the form of line-printer plots of sections through the unit cell displaying different characters (letters and numbers) that distinguish between regions within and outside the pores, respectively.

3. Variables used in the *SOLV* routine

The *SOLV* routine allows the user to choose values (to be given in Å) for the variables r_i, Δr and s. The meaning of these parameters and their influence on the calculated pore volumes $V^{\rm p}$ is described in following paragraphs.

(i) r_i is the radius attributed to the host atoms. The input instruction is `VDWR`. Since for most microporous materials the pores are confined by the surfaces of oxygen atoms, only the oxygen radius r(O) will be considered here. The interaction between the host oxygen atoms and the guests is of van der Waals, hydrogen-bond or ionic type. A value of r(O) = 1.35 Å is proposed in the *Atlas of Zeolite Framework Types* (Baerlocher *et al.*, 2001) and has been used by Marler (1989). We have chosen this value for r(O) in the following calculations to facilitate comparison between pore volumes calculated with Marler's and Spek's method. Normally, Si atoms have no part in determining the surfaces of the pores. Therefore, a radius that is sufficiently small has to be chosen for Si instead of the default value of the van der Waals radius (1.40 Å). A value of r(Si) = 0.5 Å was found to be suitable. The same value (0.5 Å) was used for the radii of host atoms Al, P and Mn to obtain the results listed in Table 1.

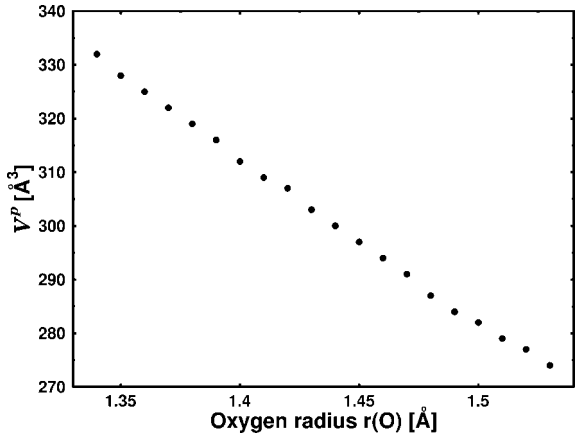

Figure 3
Pore volume $V^{\rm p}$ (Å^3) of the [$5^8$6^{12}] cage of nonasil *versus* host oxygen atom radius r(O) (Å). Δr = 1.2 Å, s = 0.12 Å.

In order to demonstrate the variation of $V^{\rm p}$ as a function of r(O), the volume of a specific pore, the [$5^8$6^{12}][1] cage in the boron-containing nonasil, |($C_4H_{10}N$)| [$Si_{21}BO_{44}$] (Marler & Gies, 1995), has been calculated for different values of r(O). The results are plotted in Fig. 3. Theoretically, the relation between $V^{\rm p}$ and r(O) is of third order. Because of the small r range, 1.34 Å $\leq r$(O) $\leq$ 1.53 Å, considered here, the curve appears to be almost linear.

(ii) Δr is the probe radius as described above (input instruction `PROBE`). Its introduction and application, as shown in Fig. 2, are the essential idea of the *SOLV* algorithm. It guarantees that only larger voids are detected and identified as pores, whereas small interstices are neglected. In the original version devoted to organic structures, Δr was fixed at 1.2 Å. To apply the *SOLV* routine to inorganic structures, in the current version of the program, Δr is allowed to vary. The default value is 1.2 Å.

If a value of Δr is chosen that is too large, small pores, which might be of interest, will not be found. If, instead, a value of Δr is used that is too small, neighbouring CGPs may coalesce and cages may combine to form larger pores. Therefore, as will be discussed in §4, the value of Δr has to be chosen properly with respect to the size of possible guests.

Fig. 4 shows, for the same [$5^8$6^{12}] cage of nonasil, how the calculated pore volume decreases with increasing Δr, because

[1] [$5^8$6^{12}] is the notation for a polyhedron confined by eight pentagons and twelve hexagons.

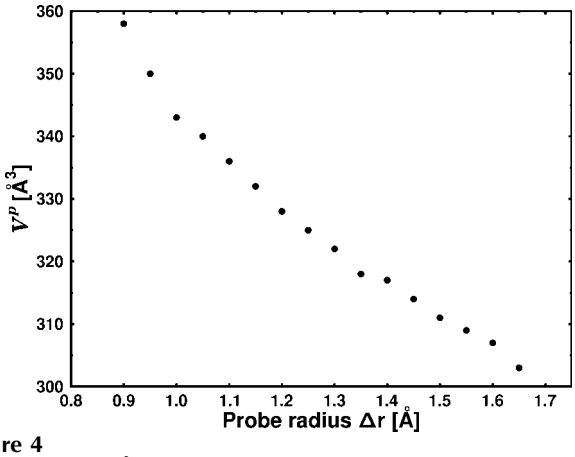

Figure 4
Pore volume $V^{\rm p}$ (Å^3) of the [$5^8 6^{12}$] cage of nonasil *versus* probe radius Δr (Å). r(O) = 1.35 Å, s = 0.12 Å.

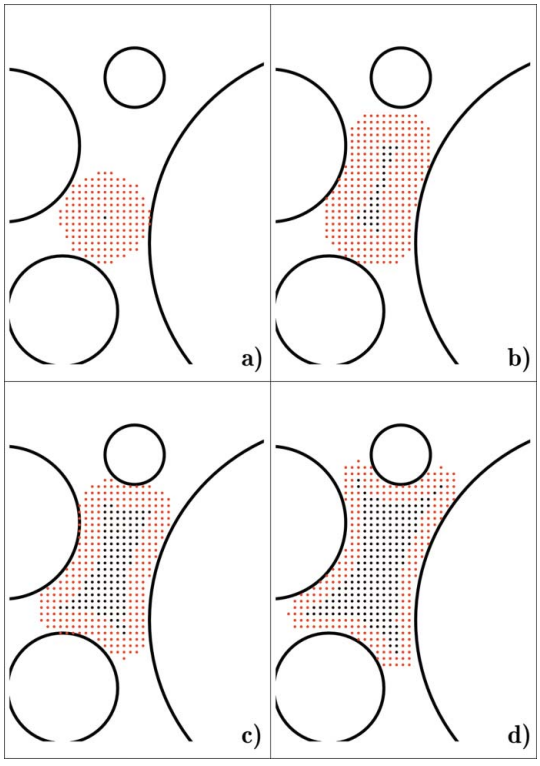

Figure 5
Two-dimensional illustration of the influence of probe radius Δr on the shape of a pore. (*a*) Δr = 1, (*b*) Δr = 0.83, (*c*) Δr = 0.55, (*d*) Δr = 0.42 (arbitrary units).

protrusions are taken into account to a lesser degree. For Δr < 0.8 Å, neighbouring pores may coalesce and ultimately channels will arise.

Fig. 5 demonstrates the influence of a variation of Δr on the shape and volume of the same pore that was used as an example in the hypothetical two-dimensional structure of Fig. 2. In Fig. 5(*a*), Δr was chosen such that the primary CGP consisted of one point only. Consequently, the augmented CGP is a circle that contacts the three nearest atom circles. In Figs. 5(*b*), 5(*c*) and 5(*d*), Δr is reduced by a factor of 0.83, 0.55 and 0.42, respectively. Thus, the pore is successively probed

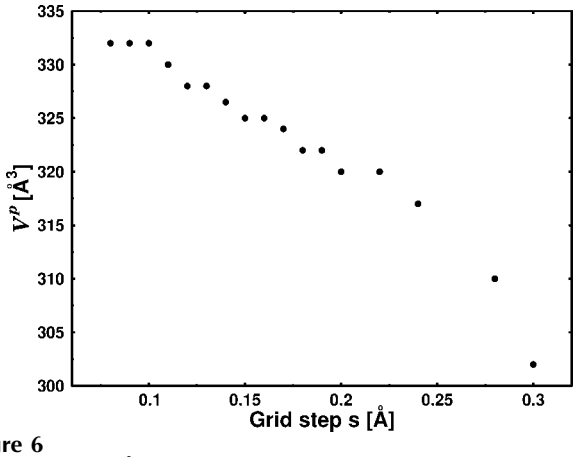

Figure 6
Pore volume $V^{\rm p}$ (Å^3) of the [$5^8 6^{12}$] cage of nonasil *versus* grid step s (Å). r(O) = 1.35 Å, Δr = 0.12 Å.

and protrusions are taken into account so that the pore volume increases.

(iii) The 'grid step' s determines the mesh size of the superimposed grid. The value of s is controlled by an input instruction `GRID` (default value = 0.2 Å). The effective grid step s is calculated by the program on the additional condition that the number of grid points along the three axes is a multiple of 12, allowing for exact symmetry of the grid for all space groups. Thus, the grid steps in the three axial directions are sometimes not exactly equal but may deviate slightly from the value chosen by the `GRID` instruction.

The finer the grid, the smoother the surface of a CGP and the closer the CGP touches the surfaces of the spheres representing the host atoms. Therefore, decreasing the grid step will increase slightly the calculated volume of the pore, which will converge ultimately to a limiting value. Simultaneously, the computing time will increase considerably. A value of `GRID` = 0.12 Å, which is smaller than the default value of 0.2 Å, seems to be an acceptable compromise and has been used in the following calculations. Typical computing times, using a standard PC, are, depending on the size of the unit cell, in the range of a few minutes.

Fig. 6 shows, again for the [$5^8 6^{12}$] cage of nonasil, the dependence of $V^{\rm p}$ on the grid step s.

4. Application of *SOLV* to inorganic microporous phases

We have applied the *SOLV* program to several microporous materials. The resulting pore volumes are listed in Table 1 and are compared with results, if available, derived using the 'Marler method'. The upper part of the table contains clathrates followed by zeoates, both with tetrahedron host frameworks. Finally, two zeoate-[6] structures are listed as examples of framework structures consisting of corner- and edge-sharing [MnO_6] octahedra (tunnel structures). The pores are classified according to their dimensionality $D^{\rm p}$. The column Δr lists the probe radius values used for the calculation for the particular structure. Normally, a value of Δr = 1.2 Å (default

Table 1
Pore volumes V^{p} (Å^3), number of symmetrically equivalent pores per unit cell and pore dimensionalities D^{p} for different poroates as derived by *SOLV* and by the Marler method.

n.d. = not determined. The IZA code is the short-hand designation assigned to a poroate framework type by the International Zeolite Association (IZA) (Baerlocher *et al.*, 2001). Remarks in column 3 contain information on the specific material used for the calculations. In particular, element symbols in parentheses indicate which cations occupy the tetrahedral positions of the host framework. Space-group symbols and references given in columns 4 and 5 refer to the specific material used for the calculations. Δr is given in Å.

					V^{p} (*SOLV*)					
Type	IZA code	Remarks	Space group	Ref.	$D^{p}=3$	$D^{p}=2$	$D^{p}=1$	$D^{p}=0$	Δr	V^{p} (Marler)
Clathrates-[4]	MTN	D3C (Si)	$F\bar{4}3d$	(1)				8 × 242, 16 × 102	1.3	8 × 180, 16 × 100
	DOH	D1H (Si)	$P6/mmm$	(2)				1 × 384, 2 × 114, 3 × 105	1.2	1 × 280, 2 × 90, 3 × 100
	NON	Nonasil (Si,B)	$Cmca$	(3)				4 × 328, 8 × 26, 8 × 25	1.2	4 × 210, 8 × 20, 8 × 20
	SOD	(Si)	$Im\bar{3}m$	(4)				2 × 186	1.3	2 × 166
	SOD	(Al)	$Im\bar{3}m$	(5)				2 × 236	1.35	2 × 214
	AFG	(Al,Si)	$P31c$	(6)				2 × 476, 4 × 103, 2 × 96	1.35	n.d.
	AST	(Al,P)	$F23$	(7)				4 × 308, 4 × 7	1.2	4 × 232, 4 × 8
Zeoates-[4]	TON	ZSM-22 (Si)	$Cmc2_1$	(8)			2 × 171		1.2	2 × 118
	RTE	Decasil (Si)	$C2/m$	(9)			2 × 306	2 × 22	1.2	n.d.
	DDR	D3R (Si)	$R\bar{3}m$	(10)		3 × 722		9 × 97, 6 × 40	1.35	6 × 300, 9 × 100, 6 × 40
	FER	(Si)	$Immm$	(11)		2 × 380			1.2	n.d.
	ISV	ITQ-7(Si)	$P4_2/mmc$	(12)	2100			4 × 23, 4 × 19	1.2	n.d.
	BRE	(Al,Si)	$P2_1/m$	(13)		2 × 207			1.2	n.d.
	FER	(Al,Si)	$I222$	(14)		2 × 424			1.2	n.d.
	LTA	(Al,Si)	$Fm\bar{3}c$	(15)	7335			8 × 193, 24 × 12	1.2	7384, 8 × 135
Zeoates-[6]	–	$Rb_{0.19}MnO_2$	$I4/m$	(16)			2 × 20		1.2	2 × 13
	–	$Rb_{0.27}MnO_2$	$A2/m$	(17)			2 × 98		1.2	2 × 76

References: (1) Gies (1984); (2) Gies (1986*b*); (3) Marler & Gies (1995); (4) Knorr *et al.* (1998); (5) Depmeier & Bührer (1991); (6) Ballirano *et al.* (1997); (7) Bennett & Kirchner (1991); (8) Marler (1987); (9) Marler *et al.* (1995); (10) Gies (1986*a*); (11) Gies & Gunawardane (1987); (12) Villaescusa *et al.* (1999); (13) Cabella *et al.* (1993); (14) Yokomori *et al.* (2001); (15) Gramlich & Meier (1971); (16) Yamamoto *et al.* (1990); (17) Tamada & Yamamoto (1986).

value) was used. In some cases, however, the resulting pore dimensionality was higher than that usually assigned to the particular structure (see the following paragraphs with afghanite as an example). In such cases, a value of $\Delta r > 1.2$ Å was used. As expected, the V^{p} values derived with *SOLV* are, in general, higher than the corresponding 'Marler values', because protrusions of the pores are taken into account by *SOLV* but not by the Marler method. In a few (three) cases, Marler volumes were slightly larger than the corresponding *SOLV* volumes. This may happen when the pore has depressions instead of protrusions.

In the following, we use afghanite as an example to demonstrate the ability of the *PLATON*/*SOLV* program to explore various properties of poroates, such as the pore dimensionality with respect to a given guest, diffusion paths in zeoates and the aperture of windows within a pore wall. Afghanite is chosen because it is an intricate example and exhibits various complications and potential pitfalls arising during the study of a poroate.

Afghanite, $|Ca_{10}(Na,K)_{22}(SO_4)_6Cl_6|$ $[Si_{24}Al_{24}O_{96}]$ (Ballirano *et al.*, 1997), is trigonal (space group $P31c$). Its structure (Fig. 7) can be regarded as being made up of three structural columns running parallel to [001] in each unit cell. These columns are designated I, II and II′. Column I consists of four cancrinite cages C, $[4^6 6^5]$, per lattice constant c_0, which are stacked along $[00z]$ in the sequence C1–C2–C1′–C2′ (C1′ is symmetrically equivalent to C1, and C2′ is symmetrically equivalent to C2, by the action of a glide plane c). Each of the two other (mutually symmetrically equivalent) columns II (at $[\frac{2}{3}\ \frac{1}{3}\ z]$) and II′ (at $[\frac{1}{3}\ \frac{2}{3}\ z]$), consists of one cancrinite cage C3

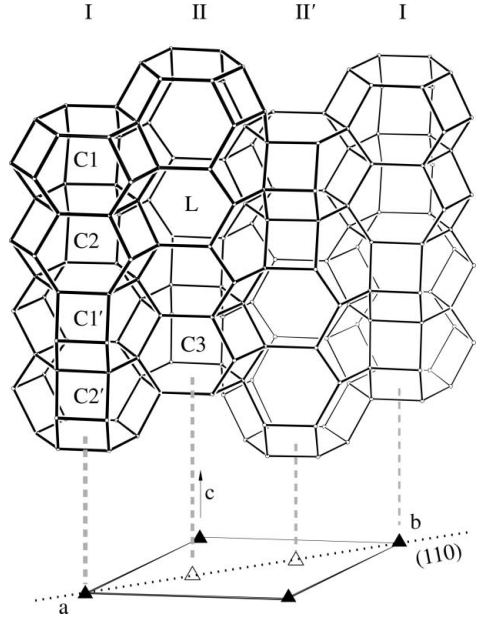

Figure 7
Schematic representation of the structure of afghanite, $|Ca_{10}(Na,K)_{22}(SO_4)_6Cl_6|$ $[Si_{24}Al_{24}O_{96}]$. C_1, C_2 and C_3: cancrinite cages $[4^6 6^5]$. L: liottite cage $[4^6 6^{17}]$.

and one large liottite cage L, $[4^6 6^{17}]$, of approximately three times the height of a cancrinite cage. The cages within each column share common, nearly planar rings of six $[(Al,Si)O_4]$ tetrahedra ('6-rings'). The columns I, II and II′ are mutually interconnected by puckered 6-rings, thus building the three-dimensional host framework.

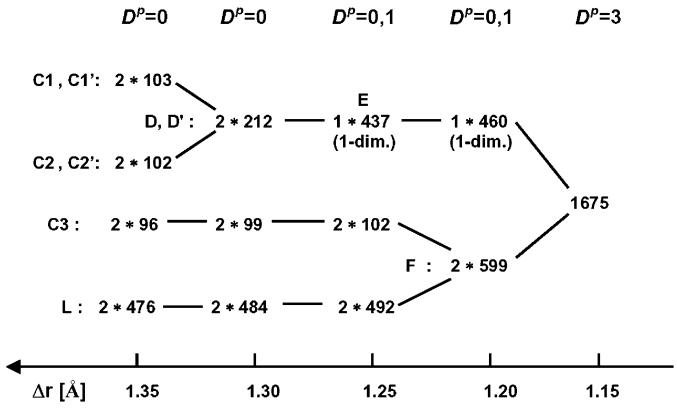

Figure 8
Pore volumes (Å^3) and pore dimensionalities D^p for afghanite as a function of probe radius Δr.

In Fig. 8 the pore dimensionalities D^p and the pore volumes V^p of afghanite are summarized as a function of the probe radius Δr. The result demonstrates that the dimensionality of the pores changes from zero-dimensional *via* one-dimensional to three-dimensional if Δr decreases. If Δr has a value of 1.35 Å (which is approximately equivalent to the radius of a K^+ ion), each of the constituting pores is recognized as a separate cage. If Δr is lowered to 1.30 Å, pairs of cages, C1 and C2, and C1′ with C2′, coalesce into larger cages, C1 + C2 → D and C1′ + C2′ → D′, with approximately twice the volume of a former cage. If Δr is lowered to a value of 1.25 Å, the cages D and D′ coalesce into a one-dimensional channel E parallel to [001]. If Δr is further reduced to a value of 1.20 Å, the cages C3 and L of column II (and II′) merge into a larger pore F. The question whether this coalescence leads to a cage or a channel parallel to [001] cannot be answered from the mere numerical value of the pore volume. More detailed analyses, which are described in a later paragraph, will show that F is a zero-dimensional pore, *i.e.* a cage. If Δr is lowered even further to a value of 1.15 Å (which is approximately equal to the radius of a Na^+ ion) the cages F merge into channels parallel to [001] and, in addition, puckered 6-rings between different columns become permeable. Thus, for guests with radii less than 1.15 Å, afghanite has a three-dimensional channel system.

These considerations make clear that the parameter Δr represents the radius of a, supposedly spherical, guest individual. If Δr is continuously reduced such that, at a certain critical value Δr_{crit}, the primary CGPs of two neighbouring cages have at least one grid point in common, then the two cages will, after the extension to the augmented CGP, coalesce into one larger pore. This demonstrates that a continuous variation of Δr allows one to estimate the penetrability of a window by the determination of a maximum diameter of a spherical guest that is able to penetrate the window. Furthermore, one can determine diffusion paths for spherical guests of radius $r = \Delta r$. This aspect will be treated in more detail in the following paragraphs.

Fig. 8 shows that the dimensionality of the pores of a poroate, and therefore its classification as a clathrate or zeoate, depends on the size of the guest species under consideration. The same material may behave as a clathrate with respect to large guests and as a zeoate for smaller guests. This aspect has been shown already by Gies (1986*a*) for the poroate D3R, which was synthesized with 1-aminoadamantane as structure-directing agent (template). D3R is a clathrate with respect to this rather large guest molecule. It is a zeoate, however, with respect to the thermal decomposition products of 1-aminoadamantane.

As described above, *SOLV* provides a plotting routine, *LIST*, which allows one to visualize the pores by line-printer plots of sections taken through the unit cell. These plots are particularly suitable to show the shape of the pores and to visualize diffusion paths in zeolites. The *SOLV* routine allows sections to be drawn only parallel to the planes (100), (010) and (001). In the case of afghanite, however, the section parallel to (110) is most instructive to illustrate the various merging processes discussed above. Fig. 7 shows that this section contains the central axes of the three columns I, II and II′ and leads from one corner of the unit cell (black triangle in the left part of Fig. 7) through the threefold axes within the unit cell (white triangles at $[\frac{2}{3}\ \frac{1}{3}\ 0]$ and at $[\frac{1}{3}\ \frac{2}{3}\ 0]$) to the black triangle in the right part of Fig. 7.

Since *LIST* cannot plot sections parallel to (110), the trigonal unit cell was transformed into a triclinic unit cell (space group $P1$) that has the direction $[\bar{1}10]$ as unit vector $\mathbf{a}'$ according to the transformation matrix

$$\begin{pmatrix} -1 & 1 & 0 \\ 0 & 1 & 0 \\ 0 & 0 & 1 \end{pmatrix}.$$

A series of plots parallel to (110) (referred to the trigonal cell) is shown in Figs. 9(*a*)–9(*f*) for different values of Δr. The printed plots have been modified in order to improve clarity. In the original line-printer plots, as generated by *LIST*, the grid points that belong to different pores are represented by different capital letters. These capitals have been replaced by differently coloured rectangles. Identical colour has been given to pores that are equivalent according to space-group symmetry.

Since, in the line-printer plots, the distances of the characters and the line width can be varied only in discrete steps, the metrics of the unit cell can be reproduced only approximately. In our example, the ratio of the axes in the plot $[(a'/c)_{plot} = 1.06]$ approximately equals the ratio of the axes of the triclinic unit cell (a'/c_0 = 22.17 Å/21.41 Å = 1.04).

In order to enable the reproduction of the plots for the limited space in a journal, it was necessary to use a rough grid with grid step s = 0.22 Å (96 grid points per lattice constant). Thereby, resolution is reduced and the boundaries of the pores are roughly stepped.

If, with varying Δr, two pores coalesce into one larger pore, *i.e.* if the window between the two pores becomes permeable, the pores will be represented by the same colour. Thus, the permeability of a window becomes visible.

In the plots of Fig. 9, Δr is varied between 2.00 Å and 1.15 Å. In Fig. 9(*a*), which is obtained from a calculation with a probe radius Δr = 2.00 Å and which should be compared with

Fig. 7, separate cancrinite cages (C1, C2 and C3) and liottite cages (L) are visible. The different colours indicate that these pores are, in fact, cages. If the size of a potential guest is reduced by setting Δr to 1.35 Å, more details of the shape of the pores become visible (Fig. 9*b*). Neighbouring cages come into contact with each other, but the 6-ring windows between them are not yet permeable. This is indicated by different colours. At Δr = 1.30 Å (Fig. 9*c*), the 6-ring window between C1 and C2 has become permeable as shown by the same colour of the two cages, which now build a larger cage, D. Correspondingly, the two cages C1′ and C2′, which are symmetry equivalent to C1 and C2, merge into the larger cage D′. These cages D and D′ are in contact with each other, but they are not yet connected by a permeable window, as indicated by different colours. D and D′ are symmetrically equivalent and should have, according to the above-mentioned convention, the same colour. However, in order to emphasize that they do not form one common pore, slightly different colours have been given to D and D′, namely dark blue (D) and light blue (D′). For guests with further reduced radius of 1.25 Å (Fig. 9*d*), the common 6-ring window between the two cages D and D′ becomes permeable, and the pore becomes a one-dimensional channel E, parallel to [001]. For Δr = 1.20 Å (Fig. 9*e*), the colours of the cages L and C3 in Fig. 9(*d*) become the same. This is not necessarily an indication that a one-dimensional channel parallel to [001] has been formed. The upper part of cage L in Fig. 9(*d*) must necessarily have the same colour as the lower part, L′, because both parts are equivalent by translational symmetry (it is 'the same' cage!). The same argument applies in Fig. 9(*e*) to the corresponding regions F and F′. When in Fig. 9(*e*) the column II shows the same colour throughout, this may result from the fact that only one of the two windows, w1 or w2 (Fig. 9*e*), which are not symmetry equivalent, has become permeable. It turns out (see next paragraph) that, in fact, only one window (the upper one, w1) has become permeable to spherical guests of radius Δr = 1.20 Å, but not the other. This means that the two cages L and C3 have merged into one larger cage F and not into a channel. In order to indicate that F is a cage and not a channel, slightly different colours (red and pink) have been given to the upper and lower cages F and F′.

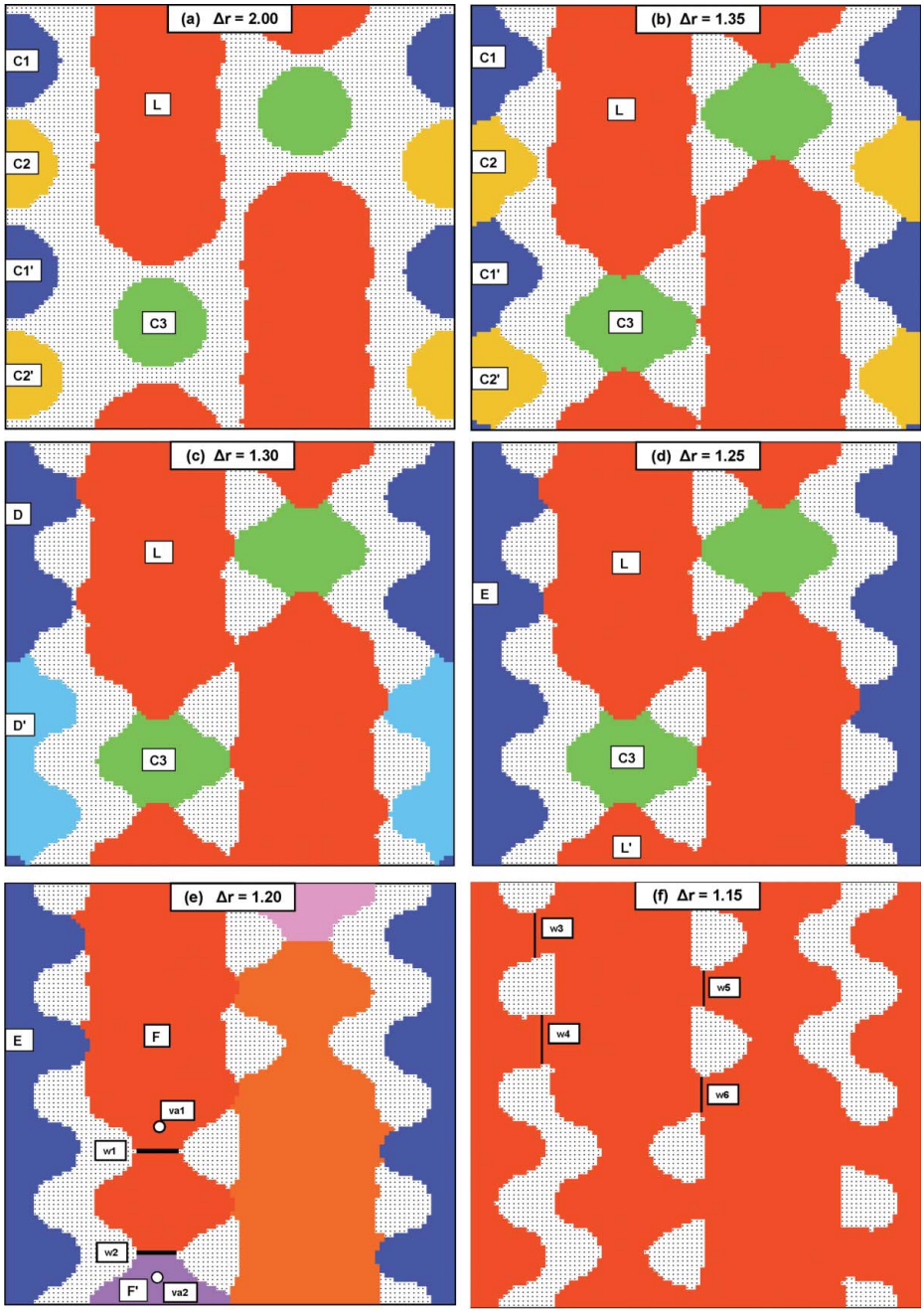

Figure 9
Plots of the (110) section through the afghanite structure, indicated in Fig. 7 by a dotted line, calculated with different probe radii Δr. Symmetrically equivalent pores are represented by the same or similar colour.

To check the penetrabilities of the windows w1 and w2, the following procedure has been applied. A virtual atom, va1, is inserted into cage L of Fig. 9(*d*) at a position that is indicated in Fig. 9(*e*) by a white circle. This virtual atom will act to block the window w1. The subsequent calculation yielded two separate cages (L and C3). This result means that the lower window w2 is not yet permeable at Δr = 1.20 Å. If, instead of va1, another virtual atom, va2 (white circle in the lower part of Fig. 9*e*), is inserted, the calculation yields one cage (F)

composed of the former cages L and C3. This means that only window w1 is permeable at Δr = 1.20 Å.

In order to determine at which value of Δr the window w2 becomes permeable, Δr was reduced almost continuously. This occurred at Δr = 1.195 Å.

At Δr = 1.15 Å (Fig. 9*f*), the whole pore space is represented by the same colour. This means that for guests with radii less than 1.15 Å, the pores have coalesced into a three-dimensional channel system and that at least one of the symmetrically non-equivalent 6-ring windows w3, w4, w5 or w6 between adjacent columns I, II and II′ has become permeable. In order to determine the permeability of these windows, again virtual atoms were inserted at the appropriate places and Δr was varied almost continuously. The resulting probe radii Δr, for which these windows become permeable, are listed in Table 2.

In order to visualize the complete shape of the three-dimensional space that is available to spherical guests for a diffusion path, a stack of sections parallel to each section shown in Figs. 9(*a*)–9(*f*) has to be plotted.

The preceding considerations suggest that it is necessary to clarify the meaning of the term 'size (synonymously: opening, width or aperture) of a window' as used in the literature.

Most authors characterize the ring width using one or more 'diameters' (Baerlocher *et al.*, 2001; McCusker *et al.*, 2001; Liebau, 2003), each of which is defined as the length of a line which connects two opposite atoms of the ring, reduced by the sum of their van der Waals or ionic radii. Such a definition seems to be suitable only if the ring is planar and consists of an even number of atoms. If the ring is not planar, such 'diameters' do not intersect and are unsuitable to function, *e.g.* as axes of an ellipse or a circle, which represent the size of a window.

With regard to practical applications, all these 'diameters' are intended to serve as a means to judge the penetrability of the windows. The question of the penetrability is, however, readily answered by the present *PLATON*/*SOLV* approach, without introduction of pore diameters, the use of which is questionable. The continuous variation of the probe radius Δr leads to a maximum radius of a sphere that is able to penetrate the window. The radius of this sphere should be used, therefore, as a measure of the size of a window, as was done in the previous study of afghanite. In the *PLATON*/*SOLV* method, the geometry of the arrangement of atoms making up a ring, which is common to two pores, or a bottleneck of a channel, may deviate considerably from planarity. A 'rolling sphere' of radius Δr will find its way even if the diffusion path is curved or arbitrarily wound.

Nevertheless, values of 'free diameters' of a ring, as given in the *Atlas of Zeolite Framework Types* (Baerlocher *et al.*, 2001), and of metrical ring widths ($W_1^R \leq W_2^R$), as defined by Liebau (2003, pp. 36f and 55 therein), can give some suitable clues on diffusibility in the case of guests which deviate considerably from spherical shape. The probe radius Δr used in the *SOLV* routine corresponds to the minimum 'free diameter' and to the minimum metrical ring width W_1^R, respectively. In order to obtain information about the length of the other (longer) 'free diameters' or the maximum ring width W_2^R, sections as in Fig. 9 have to be drawn. The lengths of these diameters and of W_2^R can then be calculated from the coordinates of relevant grid points.

Table 2
Maximum radii (Å) of spheres that are able to penetrate the windows w1 to w6 of the afghanite framework (see Figs. 9*e* and 9*f*).

Window	w1	w2	w3	w4	w5	w6
Δr (Å)	1.230	1.195	1.116	1.185	1.121	1.118

An additional remark should be made. In Fig. 9(*c*) one can see that the red area of cage L evidently covers part of the green area which belongs to cage C3. During reduction of Δr in the calculations, such a situation occurs shortly before the common window between these two cages becomes permeable, *i.e.* when the convex cages overlap and a lens-like space within the window belongs to both cages. The program *SOLV* works in such a way that the cages are filled with grid points, one after the other, in the sequence in which they are detected. Thus, each grid point is attributed to only one cage. Therefore, the space in question is allotted to the cage detected first [in the case of Fig. 9(*c*), to cage L and not cage C3]. This procedure results in slightly smaller calculated volumes for cages treated later. In cases where the exact volume of a cage is of interest, windows between this cage and neighbouring interfering cages have to be made impenetrable by inserting virtual atoms into the neighbouring cages. On the other hand, the procedure chosen in the program, namely to count the space common to two overlapping pores only once, is appropriate to calculate the porosity P according to equation (1).

The preceding discussion shows that the porosity P, as defined by equation (1), does not have a constant value for a particular host material, but depends on the size of a potential guest. As shown in Figs. 4, 5 and 9, the volume of the pores increases and the number of pores may increase if the size of the guests (*i.e.* Δr) decreases. Therefore, the total volume of the pores [numerator in equation (1)] and, consequently, P will increase.

5. Conclusions

It has been shown that the *PLATON*/*SOLV* program is well suited to determine volumes and shapes of pores in crystalline microporous materials. Furthermore, the variation of the probe radius allows extensive conclusions to be drawn concerning important properties of zeolites and zeolite-like materials. It is shown that the decision whether a material behaves as a clathrate or a zeoate depends on the size of a supposed guest. A critical size, above which a spherical guest can no longer penetrate a window between two pores can be determined. In addition, diffusion paths of spherical guests can be determined and mapped.

Thus, the *SOLV* routine is useful to simulate the diffusion behaviour of guest species in inorganic crystalline microporous materials, which is a presupposition for application of

these materials in absorption, exchange and catalytic processes.

It is shown that the porosity P does not have a constant value for a particular host material, but depends on the size of a potential guest species.

Thanks are due to Dr C. Griewatsch for providing Figs. 2 and 5, to Dr H. Katzke for manifold help, to Professor Ch. A. Geiger for improving the manuscript, and to an anonymous referee for valuable suggestions. Preliminary results of these studies have been presented at scientific meetings in Jena (Küppers & Liebau, 2004) and Rome (Liebau & Küppers, 2004).

References

Baerlocher, Ch., Meier, W. M. & Olson, D. H. (2001). *Atlas of Zeolite Framework Types*, 5th ed. Available with updates from http://www.iza-structure.org/databases/. Amsterdam: Elsevier.
Ballirano, P., Bonaccorsi, E., Maras, A. & Merlino, S. (1997). *Eur. J. Mineral.* **9**, 21–30.
Bennett, J. M. & Kirchner, R. M. (1991). *Zeolites*, **11**, 502–506.
Blatov, V. A., Blatova, O. A., Ilyushin, G. D. & Dem'Yanets, L. N. (2005). *Eur. J. Mineral.* **17**, 819–827.
Cabella, R., Lucchetti, G., Palenzona, A., Quartieri, S. & Vezzalini, G. (1993). *Eur. J. Mineral.* **5**, 353–360.
Depmeier, W. & Bührer, W. (1991). *Acta Cryst.* B**47**, 197–206.
Gies, H. (1984). *Z. Kristallogr.* **167**, 73–82.
Gies, H. (1986*a*). *Z. Kristallogr.* **175**, 93–104.
Gies, H. (1986*b*). *J. Inclusion Phenom.* **4**, 85–91.
Gies, H. & Gunawardane, R. P. (1987). *Zeolites*, **7**, 442–445.
Gramlich, V. & Meier, W. M. (1971). *Z. Kristallogr.* **133**, 134–149.
Knorr, K., Mädler, F. & Papoular, R. J. (1998). *Microporous Mesoporous Mater.* **21**, 353–363.
Küppers, H. & Liebau, F. (2004). *Z. Kristallogr. Suppl.* **21**, 120.
Liebau, F. (2003). *Microporous Mesoporous Mater.* **58**, 15–72.
Liebau F. & Küppers H. (2004). *Micro- and Mesoporous Mineral Phases*, pp. 109–112. Pre-Prints, Accademia Nazionale dei Lincei, Rome.
Marler, B. (1987). *Zeolites*, **7**, 393–397.
Marler, B. (1989). Thesis, Mathematisch-Naturwissenschaftliche Fakultät der Universität Kiel.
Marler, B. & Gies, H. (1995). *Zeolites*, **15**, 517–525.
Marler, B., Grünewald-Lüke, A. & Gies, H. (1995). *Zeolites*, **15**, 388–399.
McCusker, L. B., Liebau F. & Engelhardt, G. (2001). *Pure Appl. Chem.* **73**, 381–394.
Spek, A. L. (2005). *PLATON. A Multipurpose Crystallographic Tool*. Utrecht, University, NL, available *via* http://www.cryst.chem.uu.nl/platon (for Unix) and http://www.chem.gla.ac.uk/~louis/software/platon/ (for MS Windows).
Tamada, O. & Yamamoto, N. (1986). *Mineral. J.* **13**, 130–140.
Villaescusa, L. A., Barrett, P. A. & Camblor, M. A. (1999). *Angew. Chem.* **111**, 2164–2167.
Yamamoto, N., Oka, Y. & Tamada, O. (1990). *Mineral. J.* **15**, 41–49.
Yokomori, Y., Wachsmuth, J. & Nishi, K. (2001). *Microporous Mesoporous Mater.* **50**, 137–143.